

ICSO 2016

International Conference on Space Optics

Biarritz, France

18–21 October 2016

Edited by Bruno Cugny, Nikos Karafolas and Zoran Sodnik



Below Rule'07 low dark current LWIR and VLWIR MCT 2D focal plane detector arrays from AIM

M. Haiml

D. Eich

W. Fick

H. Figgemeier

et al.



icso proceedings



BELOW RULE'07 LOW DARK CURRENT LWIR AND VLWIR MCT 2D FOCAL PLANE DETECTOR ARRAYS FROM AIM

M. Haiml, D. Eich, W. Fick, H. Figgemeier, S. Hanna, M. Mahlein, W. Schirmacher, R. Thöt
AIM Infrarot-Module GmbH, Theresienstr. 2, D-74072 Heilbronn, Germany

I. INTRODUCTION

In recent years, high-operation temperature (HOT) detector applications in the mid-wave infrared spectral range (MWIR) have widely attracted attention [1, 2]. In the LWIR and VLWIR spectral ranges, an increase in operating temperature while keeping the detector performance obtained at lower temperatures proved to be significantly more difficult. The demands on detector material quality and detector processing are much higher. With LWIR HOT detector applications more and more evolving, AIM as a leader in LWIR MCT detectors has addressed the challenge. We like to note that AIM has a long standing track record on dark-current reduction, especially by extrinsic Au doping in the LWIR and VLWIR spectral range [3, 4, 5, 6]. During the last couple of years we matured our p-on-n LWIR technology, a key technology for high-performance small pixel pitch planar LWIR HOT MCT devices [9].

In this paper we present the status of our n-on-p and p-on-n low dark current planar MCT photodiode technology. The development was funded by ESA TRP contracts and resulted in follow-on contracts to even further optimize LWIR and VLWIR MCT and corresponding ROICs, especially for low-temperature, large area, astronomy applications.

AIM's manufacturing of HOT MCT devices is based on the liquid phase epitaxial (LPE) growth on lattice-matched in-house grown CdZnTe (CZT) substrates from a Te-rich melt, using the vertical dipping method [7, 8]. This method allows growing large MCT wafers with currently fair homogeneity in layer thickness ($\pm 1\mu\text{m}$) as well as in composition ($\pm 0.3\mu\text{m}$ cut-off wavelength) across an area of 1.5 inch diameter in the LWIR-VLWIR cut-off wavelength range.

We have investigated and compared technological constraints and performance of n-on-p and p-on-n growth for different doping levels and other process parameters. In the following we present the results for both technologies on 512 x 320 pixel format arrays with 20 μm pixel pitch.

P-ON-N TECHNOLOGY

Fig. 1 shows the thermal dark current density versus inverse detector operating temperature for p-on-n planar photodiode LWIR and VLWIR MCT detector devices. The temperature scale is normalized with respect to the cut-off wavelength for easier comparison.

At about 80K operating temperature, we measure dark current densities of $\sim 0.1\text{pA}/\mu\text{m}^2$ (FPA with 11.4 μm responsivity cut-off at 80K, dark blue curve), $\sim 0.9\text{pA}/\mu\text{m}^2$ (FPA with 11.2 μm cut-off at 80K, light blue curve) and $< 4\text{pA}/\mu\text{m}^2$ (fan-out with 11.2 μm cut-off at 80K, measured at 84K, green curve) in the 11.2-11.4 μm cut-off wavelength range (LWIR) and for two different n-type absorber doping levels. Also, the dark current behavior of the VLWIR device (fan-out with 13.1 μm cut-off @ 80K, curve in black) follows nicely the curve obtained for the LWIR device with the same doping level.

Please note that the measured dark currents are about or stay even below the values from the Tennant 'Rule 07' benchmark [10, 11] (red curve in the figure). This indicates long minority carrier lifetimes in the absorbing MCT layer.

In order to characterize the broad band photo response, the detector was operated at a 55K temperature (cut-off wavelength $\sim 11.8\mu\text{m}$) and exposed to a large area blackbody scene. For signal-to-noise improvement, a number of frames were recorded and averaged at each scene temperature.

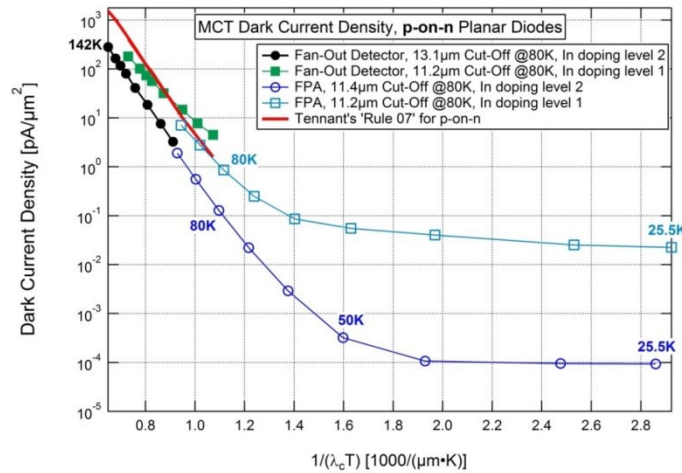


Fig. 1. Thermal dark current density versus detector operating temperature for AIM p-on-n LWIR MCT detector devices with responsivity cut-off wavelengths at 80K as stated in the inset.

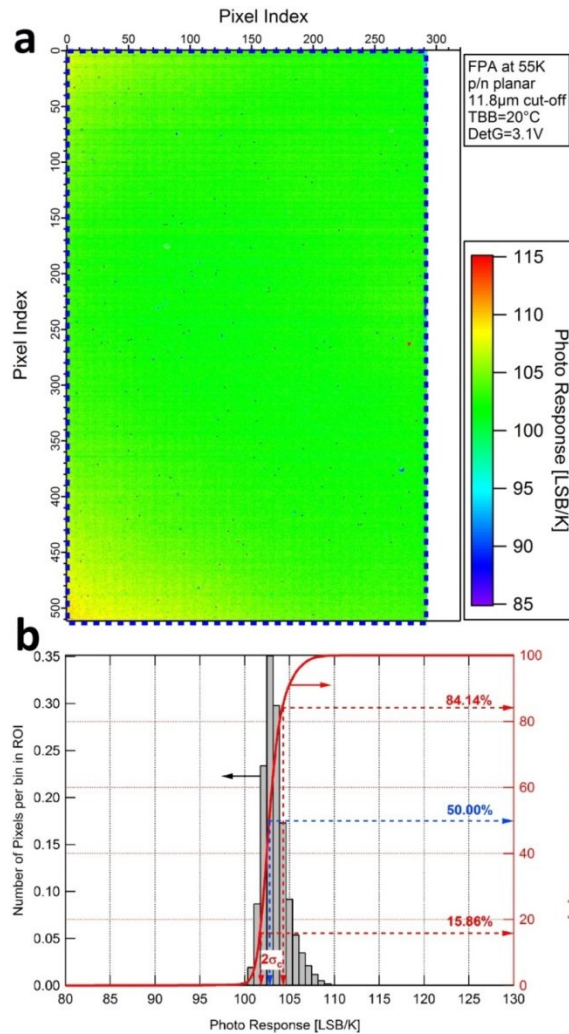


Fig. 2. (a) photo response pixel map for a p-on-n LWIR MCT FPA operated at 55K and (b) corresponding histogram.

A photo response non-uniformity of $\sigma_c/R_{med} \sim 1.2\%$ at 55K is observed for a 20°C blackbody scene illumination, and the fraction of defective pixels is only 0.2%.

Without discarding any pixels at an 80K operating temperature and an 11.0 μm QE cut-off, 0.45% of all pixels are considered defective. At 100K, the fraction of defective pixels is 2.0% at a 10.4 μm QE cut-off, and at 110K it is 3.2% at a 10.2 μm QE cut-off. Due to the increased symmetry in the NETD histograms at lower temperatures such as at 50K, we obtain only 0.20% defects at an 11.9 μm QE cut-off, and at 30K, 0.12% of the pixels are considered defective at a corresponding 12.6 μm cut-off.

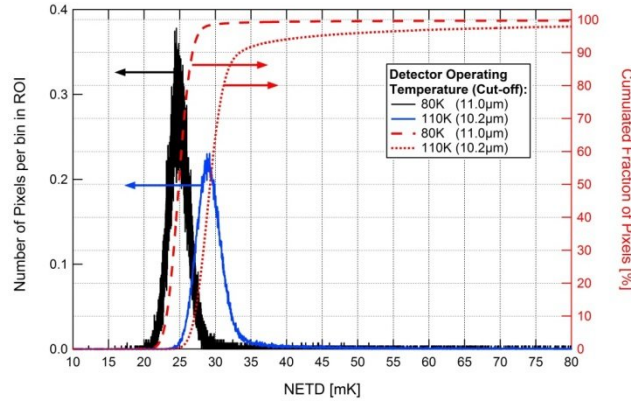


Fig. 3. NETD histograms (left axis) and cumulative histograms (right axis) for a p-on-n LWIR MCT FPA at an 80K and 110K detector operating temperature. The detector is illuminated with a 25°C large area blackbody scene at about half well filling level.

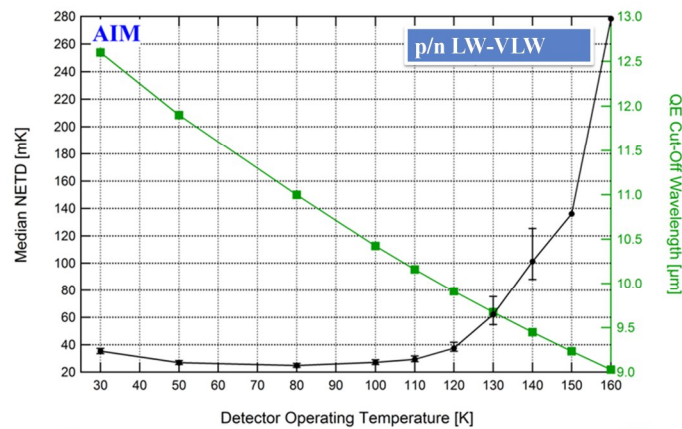


Fig. 4. cut-off wavelength (green) and median NETD (black) versus FPA temperature.

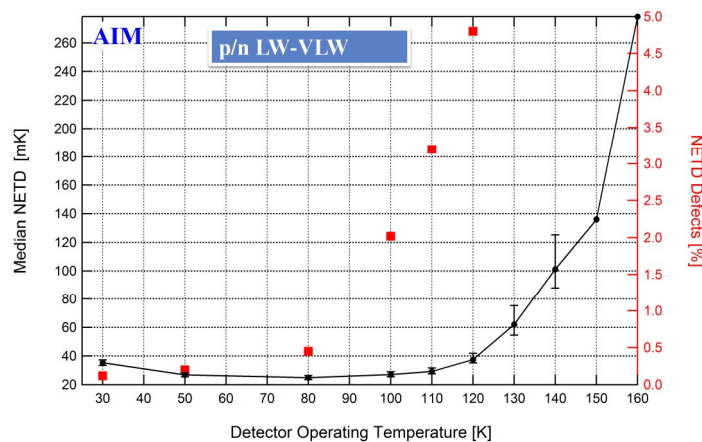


Fig. 5. median NETD (black) and NETD defects (red) versus FPA temperature. A pixel is masked defective if its NETD value is above twice or below half of the array median NETD.

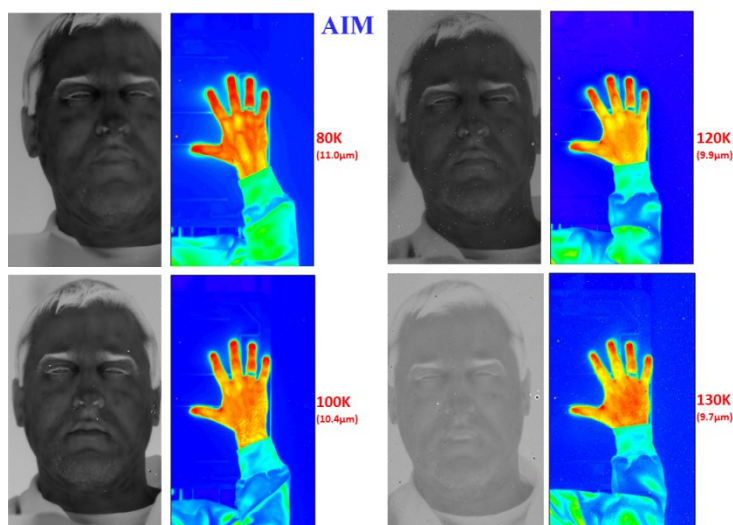


Fig. 6. Images taken with an AIM p-on-n LWIR MCT FPA of a face (2-point corrected, with bad pixel replacement) and a hand touching an object (2-point corrected, without bad pixel replacement) for detector operating temperatures between 80K and 130K. The corresponding QE cut-off wavelengths (11.0µm - 9.7µm) are stated in parentheses. The degraded contrast with the face for the 130K detector operating temperature is partially due to a non-optimum software dynamic spread setting.

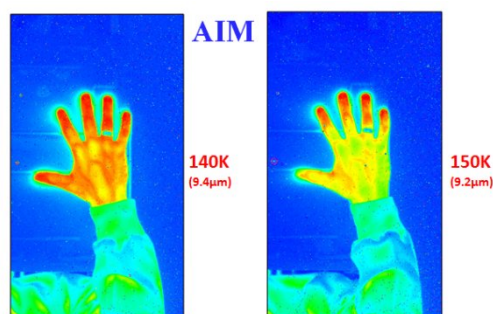


Fig. 7. Images taken with an AIM p-on-n LWIR MCT FPA of a hand touching an object (2-point corrected, without bad pixel replacement) for 140K and 150K detector operating temperatures. The corresponding QE cut-off wavelengths are stated in parentheses.

N-ON-P TECHNOLOGY

Fig. 8. shows the thermal dark current density versus inverse detector operating temperature for n-on-p planar photodiode LWIR and VLWIR MCT detector devices. The temperature scale is normalized with respect to the cut-off wavelength for easier comparison.

With the n-on-p planar diode technology approach, at 80K, we attain a 0.2-0.3pA/µm² dark current density for an 11.4-11.5µm cut-off wavelength. Thus, there is not much difference to the dark current densities from devices in p-on-n technology at 80K for comparable cut-off wavelengths. Compared to Tennant's empirical "Rule 07" established for p-on-n technology devices [10, 11], we measure dark currents lower by about a factor of three with our devices in n-on-p technology.

Notably, the measured dark current figure implies that the devices may be operated at an about 20K higher operating temperature for the same dark current level than extrinsically doped AIM n-on-p LWIR and VLWIR MCT FPAs from the previous technology generation [3, 4, 5] (dashed blue line in the figure).

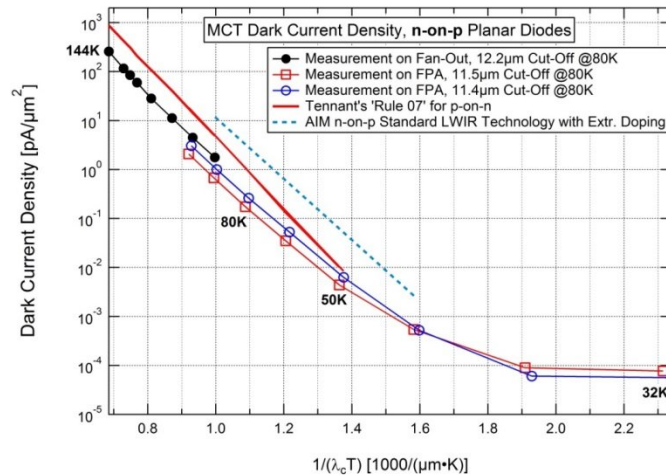


Fig. 8. Thermal dark current density versus detector operating temperature for AIM n-on-p LWIR MCT detector devices with responsivity cut-off wavelengths at 80K as stated in the inset.

The detection efficiency spectra for the FPA detector from Fig. 8 are shown in Fig. 9. The QE was measured to be slightly above 70% in the plateau for any of the set operating temperatures, which is as expected slightly larger than for the p-on-n device (60%) due to the larger minority carrier diffusion length in our n-on-p devices.

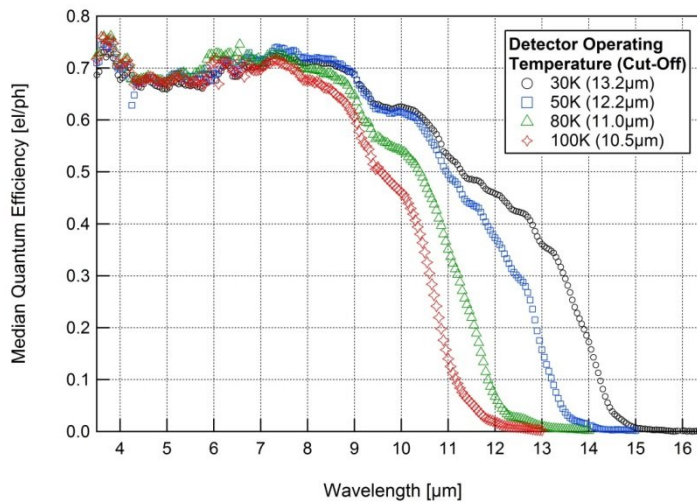


Fig. 9. Median quantum efficiency spectra for an n-on-p FPA from Figure 8 at detector operating temperatures of 30K, 50K, 80K and 100K. The given cut-off wavelengths are the wavelengths at half the maximum measured QE.

Analogous to the p-on-n devices, the photo response homogeneity of an n-on-p VLWIR MCT FPA was analyzed. The FPA under test was operated at a 55K temperature (cut-off wavelength $\sim 13.6\mu\text{m}$) and exposed to a large area blackbody scene. The F-number was 2, and the charge integration time was adjusted to attain half well filling level.

The photo response pixel map for a 20°C blackbody scene is depicted in Fig. 10. A few larger cluster defects may be discerned, which are expected to be annihilated by appropriate design measures or yield considerations, which have not been implemented here yet.

Discarding the pixels within the five largest macro defects, an excellent photo response non-uniformity of $\sigma_c/R_{\text{med}} \sim 3.1\%$ is attained at a long $13.6\mu\text{m}$ cut-off wavelength. The optical bandwidth of the detector ranges from about $3\mu\text{m}$ to $14\mu\text{m}$ wavelength in this case. The photo response non-uniformity is larger for this n-on-p FPA than for the previously considered p-on-n device mainly because the cut-off wavelength is significantly larger for the n-on-p FPA (smaller Cd mole fraction), in which case small changes in MCT stoichiometry imply a larger cut-off wavelength spread.

Discarding the pixels within the five largest macro defects, the moderate fraction of $\sim 0.75\%$ of the pixels is regarded as defective.

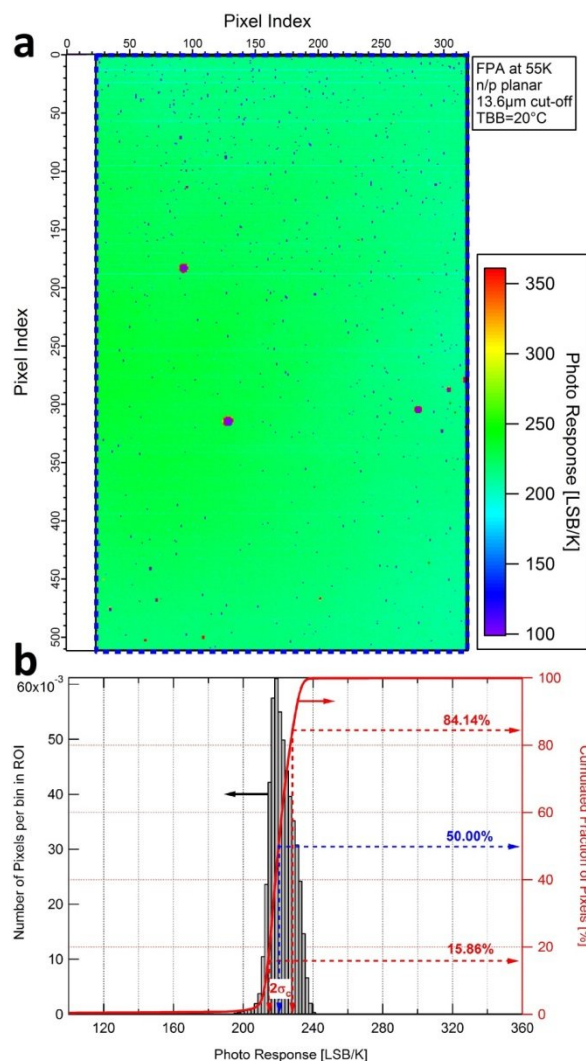


Fig. 10. (a) photo response pixel map for an n-on-p VLWIR MCT FPA operated at 55K and (b) corresponding histogram.

A photo response non-uniformity of $\sigma_c/R_{med} \sim 3.1\%$ at 55K is observed at a long $13.6\mu\text{m}$ cut-off wavelength and for a 20°C blackbody scene illumination.

CONCLUSIONS

AIM is one of a view world-wide leading suppliers of high-performance infrared detectors and focal plane sub-assemblies [12]. This paper reports on our current status of low-dark-current p/n and n/p two-dimensional LWIR/VLWIR planar MCT technology.

Thermal dark currents significantly reduced as compared to ‘Tennant’s Rule 07’ in both diode polarities were obtained in conjunction with a good detection efficiency $\geq 60\%$ and a spectral QE dispersion around only 5% for operating temperatures between 30K and 100K. This allows for the same dark current performance at a 20K higher operating temperature than with previous AIM technology.

Thermal detector sensitivities of 29.3mK for a room temperature scene, at a 110K detector operating temperature and a $10.2\mu\text{m}$ detector cut-off wavelength were demonstrated for p-on-n MCT FPAs. In the same detector technology, the infrared image capture up to a 150K operating temperature ($9.2\mu\text{m}$ cut-off) was demonstrated with an excellent image quality up to 120K ($9.9\mu\text{m}$ cut-off) and a still reasonable quality at higher operating temperatures.

For n-on-p LWIR MCT FPAs, an NETD of 30.5mK at a 100K operating temperature and a $10.5\mu\text{m}$ cut-off wavelength was attained under the same testing conditions with an excellent infrared image quality.

ACKNOWLEDGEMENTS

Large parts of the presented work have been supported by the European Space Agency (ESA) under ESTEC contract 4000107414/13/NL/SFe.

REFERENCES

- [1] R. Wollrab, A. Bauer, H. Bitterlich, M. Bruder, S. Hanna, H. Lutz, K.-M. Mahlein, T. Schallenberg, J. Ziegler, "Planar n-on-p HgCdTe FPAs for LWIR and VLWIR Applications", *J. Electron. Mat.* 40(8), 1618-1623 (2011).
- [2] H. Lutz, R. Breiter, H. Figgemeier, T. Schallenberg, W. Schirmacher, R. Wollrab, "Improved high operating temperature MCT MWIR modules", *Proc. SPIE* 9070, 90701D (2014)
- [3] S. Hanna, A. Bauer, H. Bitterlich, M. Bruder, M. Haiml, K. Hofmann, K.-M. Mahlein, H.-P. Nothaft, T. Schallenberg, J. Wendler, R. Wollrab, J. Ziegler, "Two-dimensional VLWIR arrays for Meteosat 3rd generation", *Proc. SPIE* 7474, 747415 (2009).
- [4] S. Hanna, A. Bauer, H. Bitterlich, M. Bruder, L.-D. Haas, M. Haiml, K. Hofmann, K.-M. Mahlein, H.-P. Nothaft, T. Schallenberg, A. Weber, J. Wendler, R. Wollrab, J. Ziegler, "Two-dimensional focal plane detector arrays for LWIR/VLWIR space and airborne sounding missions", *Proc. SPIE* 7826, 78261H (2010).
- [5] D. Hübner, S. Hanna, R. Thöt, K.U. Gassmann, M. Haiml, A. Weber, L.-D. Haas, J. Ziegler, H.-P. Nothaft, W. Fick, "Radiation Hardness of Two-dimensional Focal Plane Detector Arrays for LWIR/VLWIR Space Sounding Missions", *Proc. SPIE* 8533, 853311 (2012).
- [6] A. Weber, W. Belzner, L.-D. Haas, S. Hanna, K. Hofmann, A. Neef, M. Reder, P. Stifter, J. Wendler, J. Ziegler, H.-P. Nothaft, "Infrared focal plane detector modules for space applications at AIM", *Conference on Radiation Effects on Components and Systems (RADECS)* 2011.
- [7] M. Bruder, H. Figgemeier, L. Palm, J. Ziegler, H. Maier, *Proc. SPIE* 2554, 137 (1995)
- [8] H. Figgemeier, M. Bruder, K. Mahlein, R. Wollrab, J. Ziegler, "Impact of critical processes on HgCdTe diode performance and yield", *J. Electron. Mater.* 32, 588 (2003)
- [9] M.A. Kinch, "*Fundamentals of Infrared Detector Materials*", SPIE Press, Bellingham/Washington, USA (2007)
- [10] W.E. Tennant, D. Lee, M. Zandian, E. Piquette, M. Carmody, "MBE HgCdTe Technology: A Very General Solution to IR Detection, Described by "Rule 07", a Very Convenient Heuristic", *J. Electron. Mater.* 37, 1406 (2008)
- [11] W.E. Tennant, "Rule 07 Revisited: Still a Good Heuristic Predictor of p/n HgCdTe Photodiode Performance?", *J. Electron. Mater.* 39, 1030 (2010)
- [12] W. Fick, K.U. Gassmann, L.-D. Haas, M. Haiml, S. Hanna, D. Hübner, H. Höhnemann, H.-P. Nothaft, R. Thöt, "Infrared detectors for Space Applications", *Adv. Opt. Technol.* 2, 407-421 (2013).